Near-field spectroscopy of surface plasmons in flat gold nanoparticles

M. Achermann,[1,2,*] K. L. Shuford,[3] G. C. Schatz,[3] D. H. Dahanayaka,[4] L. A. Bumm,[4] and V. I. Klimov[2,5]

[1]Physics Department, University of Massachusetts, Amherst, Massachusetts 01003, USA
[2]Chemistry Division and Center for Integrated Nanotechnologies, Los Alamos National Laboratory, Los Alamos, New Mexico 87545, USA
[3]Department of Chemistry, Northwestern University, Evanston, Illinois 60208, USA
[4]Homer L. Dodge Department of Physics and Astronomy, University of Oklahoma, Norman, Oklahoma 73069, USA
[5]klimov@lanl.gov
[*]Corresponding author: achermann@physics.umass.edu

Received March 9, 2007; revised May 18, 2007; accepted May 21, 2007;
posted June 5, 2007 (Doc. ID 80883); published July 27, 2007

We use near-field interference spectroscopy with a broadband femtosecond, white-light probe to study local surface plasmon resonances in flat gold nanoparticles (FGNPs). Depending on nanoparticle dimensions, local near-field extinction spectra exhibit none, one, or two resonances in the range of visible wavelengths (1.6–2.6 eV). The measured spectra can be accurately described in terms of interference between the field emitted by the probe aperture and the field reradiated by driven FGNP surface plasmon oscillations. The measured resonances are in good agreement with those predicted by calculations using discrete dipole approximation. We observe that the amplitudes of these resonances are dependent upon the spatial position of the near-field probe, which indicates the possibility of spatially selective excitation of specific plasmon modes.

OCIS codes: 180.5810, 300.0300, 320.0320.

Metal nanostructures exhibit large polarizabilities resulting from collective electron oscillations known as surface plasmons (SPs). Excitation of SPs produces large enhancement of local fields, which has been widely utilized in surface-enhanced Raman spectroscopy [1]. Further, using SPs one can produce significant concentration of electric fields in nanosized hot spots. For example, chains of self-similar nanospheres [2] and pairs of flat triangular nanoparticles [3] have been proposed as photonic antennas for achieving efficient coupling of far-field radiation to individual molecular components. Field enhancement in these types of complex nanostructures occurs due to excitation of high-order plasmon resonances [4]. The ability to map these resonances both spatially and spectrally is essential for understanding and eventually engineering the response of metal nanostructures to external optical fields.

Near-field optical spectroscopy is a powerful technique to obtain information about spectral and spatial distribution of plasmon modes in metal nanostructures [5–9]. One recent implementation of near-field spectroscopy involved the use of a femtosecond white-light continuum transmitted through a subwavelength aperture of a near-field scanning optical microscope (NSOM) for spatially selective excitation of SP modes. In addition to ~50 nm spatial resolution, this method provided phase sensitivity, which allowed for precise determination of both SP resonance energies and linewidths in individual and aggregated metal nanoparticles [7,8]. Here, we employ a similar technique for studies of high-order SP resonances in flat gold nanoparticles (FGNPs) of a variety of sizes and shapes.

Conventional preparation procedures result in FGNP samples with a significant polydispersity [10], which greatly complicates the analysis of SP spectral structures using traditional ensemble spectroscopic techniques. The use of single-nanoparticle near-field spectroscopy not only resolves the problem of sample polydispersity but also allows one to accurately correlate the measured SP features with sample morphology.

Here, we demonstrate that the near-field extinction spectra of FGNPs can be analyzed in terms of a coherent superposition of the NSOM-aperture field (corrected for sample absorptivity) and the field reemitted by FGNP SPs. Further, we demonstrate selective excitation of specific SP modes by controlling the spatial position of the NSOM tip on the nanoparticle. A comparison of the experimental results with simulations based on a discrete dipole approximation (DDA) indicates that the measured resonances originate from high-order SP modes.

The particles studied here [10] are 15–35 nm thick single crystals with atomically flat surfaces that range in size from approximately 500 to 2000 nm. Near-field spectroscopic studies were performed by coupling a femtosecond white-light continuum into tapered, Al-coated optical fibers with ~50 nm aper-

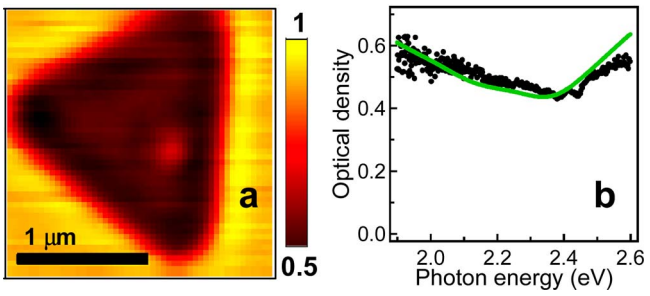

Fig. 1. (Color online) a, NSOM image of a large FGNP. b, Near-field extinction spectrum (dotted line) measured at the center of the FGNP and calculated extinction spectrum (solid line).

tures [7]. In the imaging mode, the light transmitted through the sample was collected with a photomultiplier tube while the NSOM tip was raster scanned across the sample at constant height. In the spectroscopic mode, the NSOM tip was positioned at a specific sample location and the spectrum of the transmitted light was recorded. Spectrally and spatially resolved single-nanoparticle extinction was calculated using the expression $Q=-\ln(I_T/I_{ref})$, where I_T is the near-field transmission spectrum recorded for a certain NSOM tip location above a selected FGNP and I_{ref} is the reference spectrum recorded for a nominally transparent substrate region at least 0.5 μm away from the FGNP.

We start our discussion with large FGNPs that have a characteristic lateral dimension of >1 μm. An example of such an FGNP with a thickness of 15 nm (determined from a simultaneously acquired topographic image) is shown in Fig. 1a. The FGNP appears as a dark area in the near-field transmission image. The extinction spectrum taken in the center of the particle (Fig. 1b) does not show any sharp structures, which could be related to excitation of SPs. One feature is a shallow dip around 2.35 eV. A similar dip is also found in the absorption spectrum of bulk gold suggesting that the extinction spectra of large particles are determined by bulk gold properties. Indeed, we observe a very good correspondence between the measured near-field extinction spectrum and the transmission spectrum calculated for a three-layer, air/gold/indium tin oxide (ITO) system normalized by the transmission spectrum of the air/ITO interface (solid line in Fig. 1b).

Near-field extinction spectra of small FGNPs with characteristic lateral dimensions of 0.5 μm or less (Fig. 2) are clearly different from those of larger particles. In this case, the measured extinction spectrum (Fig. 2c) and the calculated thin-film transmission

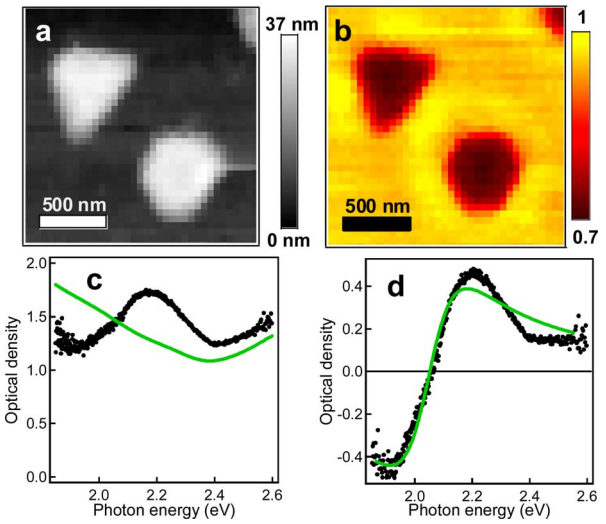

Fig. 2. (Color online) a, Topography and b, NSOM images of two small FGNPs. c, Extinction spectrum (dotted line) of the triangular particle imaged in a and b. The solid line is the calculated thin-film response. d, Spectrum after subtracting the thin-film transmission (dotted line) can be approximated by the near-field response of a single SP mode (solid line).

are significantly different indicating the importance of SP effects. Previous studies of small sub-100-nm spherical particles using a similar technique [7,8] demonstrated that near-field extinction spectra could be explained in terms of interference of the NSOM aperture field and the secondary field, E_{SP}, re-emitted by SPs excited in the nanostructure. Because of the large lateral dimensions of the FGNPs studied here ($\sim$500 nm or greater), the aperture field cannot directly reach the detector. Therefore, in our modeling, we consider not the field, E_0, directly emitted by the aperture but the field, E_T, corrected for sample transmittance. In this case, the extinction coefficient Q is

$$\begin{aligned} Q(\omega) &= -\ln\left(\frac{I_T}{I_{ref}}\right) = -\ln\left|\frac{E_T+E_{SP}}{E_{ref}}\right|^2 \\ &= -\ln\left|\frac{t(\omega)E_0+\beta t(\omega)E_0 u_{SP}(\omega)e^{i\phi(\omega)}}{E_{ref}}\right|^2 \\ &= Q_{TF}(\omega)-\ln|1+\beta u_{SP}(\omega)e^{i\phi(\omega)}|^2. \end{aligned} \quad (1)$$

Here, $t(\omega)$ and $Q_{TF}(\omega)$ are the bulklike, thin-film transmission and extinction coefficients, respectively, $u_{SP}(\omega)$ is the SP resonance line shape, and $\phi(\omega)$ is the phase shift between the driving aperture field and the field re-emitted by SPs. β is a frequency-independent proportionality factor that characterizes the efficiency of conversion of the near-field aperture radiation into the SP radiation. Because of extremely low SP radiation efficiencies, $\beta \ll 1$ and Eq. (1) can be simplified to $Q(\omega)\approx Q_{TF}(\omega)-2\beta u_{SP}(\omega)\cos(\phi(\omega))$. The latter expression indicates that the SP-related response of the FGNP, $Q_{SP}(\omega)$, can be extracted from the measured near-field spectra by simply subtracting bulklike, thin-film extinction from $Q(\omega)$: $Q_{SP}(\omega)=Q(\omega)-Q_{TF}(\omega)=-2\beta u_{SP}(\omega)\cos(\phi(\omega))$. Applying this formula to the spectral data in Fig. 2c, we obtain the spectrum shown in Fig. 2d. This bulk-background-free spectrum exhibits features typical of interference of the field emitted by the SP and the excitation field. Specifically, it shows a transition between negative and positive extinction, which occurs because of switching from constructive (below the SP resonance) to destructive (above the SP resonance) interference between the two fields [7]. The position of the zero-extinction point provides an accurate measure of the energy of the SP resonance, $\hbar\omega_{SP}$, while a line-shape analysis (based, e.g., on a simple forced harmonic oscillator model [7]) can be used for deriving the SP damping, Γ_{SP}. Specifically, based on the spectrum in Fig. 2d, we find that $\hbar\omega_{SP}=2.05$ eV and $\Gamma_{SP}=0.27$ eV. The important aspect of this single-particle method is that the measured SP features can be directly correlated with the geometry of the nanostructure under investigation and even with a specific location of the near-field excitation source.

The above analysis can also be applied to structures that exhibit multiple SP resonances. The truncated triangle shown in Fig. 3a has an interference spectrum, which suggests the presence of at least two SP modes. To determine the positions and the damp-

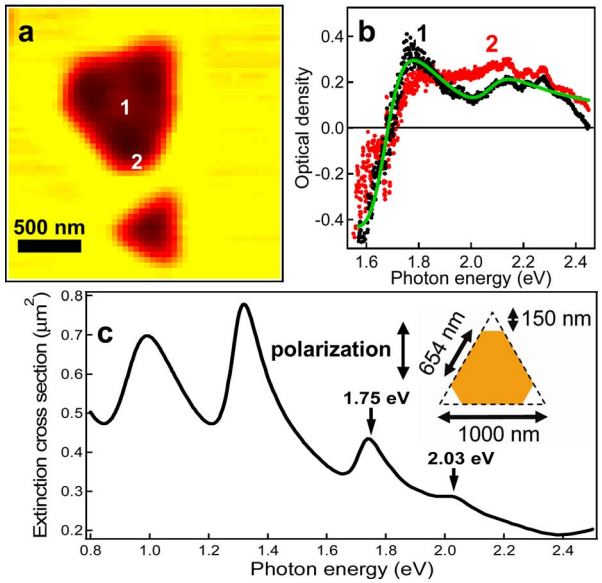

Fig. 3. (Color online) a, NSOM images of two FGNPs. b, Two near-field extinction spectra (black and red dotted lines; after subtracting the thin-film response) recorded at the positions 1 and 2 in a. These spectra can be modeled by the optical response of two independent SP modes (solid line). c, Numerical DDA calculations of the extinction spectrum of a truncated triangle (inset) for vertical polarization of the applied field (similar SP response for horizontal polarization).

ing constants of these modes, we model the SP response by two independent harmonic oscillators (Fig. 3b), which yields $\hbar\omega_{SP}=1.68$ eV and 2.07 eV and $\Gamma_{SP}=0.22$ eV for both SP modes. Because of a significant spectral separation between these two SP resonances ($\sim$0.4 eV), we neglected intermode coupling in our analysis.

An important capability of the near-field technique applied in this work is the possibility to analyze not only spectral but also spatial characteristics of SP modes in individual nanostructures. For example, we clearly see a difference in relative intensities of the two SP modes measured for the same structure but for two different positions of the NSOM probe. In the case when the near-field aperture is at the center of the structures, the SP response is dominated by the 1.67 eV mode, while, at the corner of the triangular particle, the SP spectrum is dominated by the 2.06 eV mode. These results can be qualitatively understood in terms of a difference in the spatial distribution of mode densities for the two SP resonances. Specifically, higher frequency and, hence, larger wavevector modes are expected to better penetrate into small spatial features of a nanostructure compared with lower-frequency modes. This may explain the relative enhancement of the 2.06 eV feature in the case for which the NSOM probe is positioned near the FGNP tip. These results also indicate the feasibility of spatially selective excitation of certain SP modes, which is a particularly useful capability in studies of closely separated (e.g., coupled) SP resonances.

The analysis above is in agreement with results of calculations of the spectral distribution of various modes conducted using a DDA. In this method, the FGNP is replaced with an array of point dipoles (5 nm spacing) whose polarizations are determined by the incident electrical field and by the radiation fields from the other point dipoles in the array [4]. We approximated the particle in Fig. 3a with a truncated triangle (inset of Fig. 3c). The calculated spectrum (Fig. 3c) shows two higher-order resonances with energies of 1.75 and 2.03 eV that are located in the spectral range probed in our experimental studies. The spectral positions of these resonances are in good agreement with those observed in the near-field extinction spectra (1.67 and 2.06 eV).

In conclusion, we have studied near-field extinction spectra of individual FGNPs. After subtracting a bulklike contribution from the measured extinction spectra, we derive a "pure" SP response, which shows clear signatures of interference between the aperture excitation field and the secondary field re-emitted by photoexcited SPs. By analyzing these spectra we derive spectral positions and damping constants of SPs in individual FGNPs of various morphologies. We have further studied the effect of spatially selective near-field excitation on amplitudes of different SP modes. We observe good agreement between positions of measured SP resonances and those computed using numerical DDA simulations.

G. C. Schatz and K. L. Shuford were supported by Department of Energy (DOE) grant DEFG02-02-ER15487. This work was supported by National Science Foundation (NSF) CAREER grant CHE-0239803, the Center for Physics in nanostructures, NSF (MRSEC DMR-0080054), and Oklahoma EPSCoR. Experimental studies were conducted at the Center for Integrated Nanotechnologies, a DOE Nanoscale Science Research Center operated jointly by Los Alamos and Sandia National Laboratories.

References

1. S. Nie and S. R. Emory, Science **275**, 1102 (1997).
2. K. Li, M. I. Stockman, and D. J. Bergman, Phys. Rev. Lett. **91**, 227402 (2003).
3. R. D. Grober, R. J. Schoelkopf, and D. E. Prober, Appl. Phys. Lett. **70**, 1354 (1997).
4. K. L. Shuford, M. A. Ratner, and G. C. Schatz, J. Chem. Phys. **123**, 114713 (2005).
5. T. Klar, M. Perner, S. Grosse, G. von Plessen, W. Spirkl, and J. Feldmann, Phys. Rev. Lett. **80**, 4249 (1998).
6. J. Prikulis, H. Xu, L. Gunnarsson, M. Käll, and H. Olin, J. Appl. Phys. **92**, 6211 (2002).
7. A. A. Mikhailovsky, M. A. Petruska, M. I. Stockman, and V. I. Klimov, Opt. Lett. **28**, 1686 (2003).
8. A. A. Mikhailovsky, M. A. Petruska, K. Li, M. I. Stockman, and V. I. Klimov, Phys. Rev. B **69**, 085401 (2004).
9. K. Imura, T. Nagahara, and H. Okamoto, J. Chem. Phys. **122**, 154701 (2005).
10. D. H. Dahanayaka, J. X. Wang, S. Hossain, and L. A. Bumm, J. Am. Chem. Soc. **128**, 6052 (2006).